DLSU RESEARCH CONGRESS 2020
"Building Resilient, Innovative, and Sustainable Societies"
June 17-19, 2020

Electricity Generation from Wind-Generated Waves Through Electromagnetic Induction in a Power Buoy System

Adrian Bielza[1], Godspeed Feliciano[2], Katrina Jimenez[3], Angelo Padilla[4], Eunice Uy Tan[5], Hiroki Asaba[6], Clement Ong*
[12345]*DLSU – IS SHS Department*
[6]*Computer Technology Department*
**Computer Technology Departent*
**clement.ong@dlsu.edu.ph*

Abstract: By the year 2030, the Department of Energy of the Philippines anticipates the country's demand for electricity to hit 70% more than its current capacity. In order to reach this goal, developments on current renewable energy systems should be increased since it only constitutes 25% of the current capacity. In this paper, a prototype power-buoy system consisting of permanent-magnet DC motors, a rack-pinion gear system, and a rectifier circuit was developed to utilize wave power as a source of renewable energy. The prototype also consists of power and motion measuring devices to characterize the wave and the buoy to determine its efficiency. Based on the results, the prototype showed a mechanical conversion efficiency of 37% and an electrical conversion efficiency of 15%.

Keywords: Wind-generated waves; Electromagnetic induction; Renewable energy

1. INTRODUCTION

A renewable source that has not been exploited, to date, in the Philippines is the utilization of wind-generated waves to produce electricity. The Philippines, in particular, might be well-poised to use this technology, due to its coastline length of 36,289 km. The prototype Wave Energy Converter (WEC) approach utilized in this paper is a floor-anchored buoy system as it is easier to design and develop as a prototype; however, this limits the energy conversion to the vertical component of the wave. The buoy contains a rack-pinion gear system that translates vertical motion from the waves into rotational motion that drive the DC motors. The buoy includes an accelerometer for wave displacement calculation, a full wave rectifier to convert alternating current (AC) to direct current (DC), and an Arduino for voltage measurement and data logging. Triaxial accelerometers are floated and data-logged to measure the incoming and outgoing surface waves motions. The electrical energy produced was then compared with the wave input to determine the efficiency of the system.

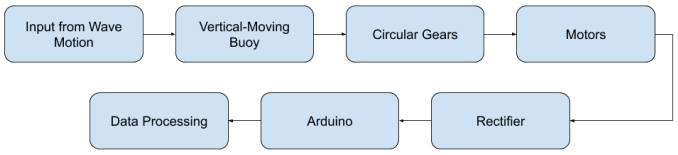

Fig. 1. Block Diagram of the Prototype

Figure 1 showcases the different components of the prototype. The vertical motion from the wave will be absorbed by the vertical-moving buoy which contains an accelerometer to measure its displacement. Through a rack-pinion gear setup, the kinetic energy absorbed by the buoy will be transferred to the circular gears attached to the motors. This will cause the motors to generate electricity, which will pass through the rectifier, converting the AC to DC. The Arduino will then record this data for post-processing on a PC.

The completed prototype is shown in Figure 2. Two canisters made of PVC pipe provide buoyancy; the platform moves only along the vertical axis, facilitated by linear guide wheels which slot into grooves cut into the square cross-sectioned mast.

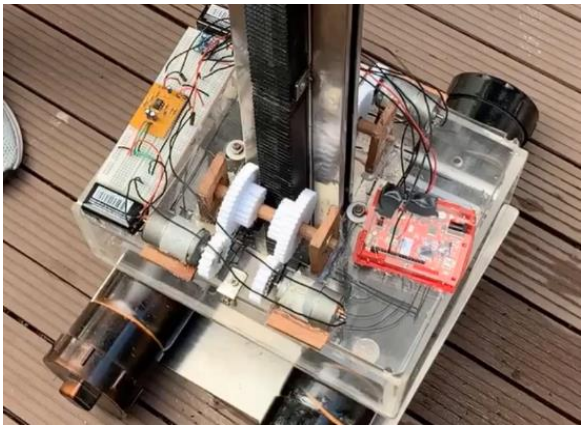

Fig. 2. Prototype Buoy. *Two stock PVC 4" pipes are plugged on each end to provide a floating platform, anchored by a mast where a ratchet has been machined. Four linear guide wheels ride on grooves in the mast to ensure smooth travel in only the vertical (up/down) direction.*

2. RESULTS

2.1 Buoy Characteristics

The power buoy prototype was initially characterized by moving the floating assembly up and down by hand, on land. The acceleration data from the MPU6050 was double integrated to acquire the displacement of the buoy.

Figure 3 shows a representative plot of motion versus output power from such test. From the graph, it was observed that power was only produced as the buoy moved up and down, with output peaks corresponding to motion at the steepest part of the graph.

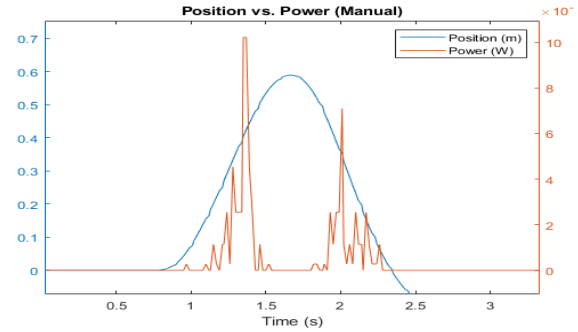

Fig. 3. Position vs. Power. *The blue graph shows the position of the buoy versus time, as integrated from the accelerometer on the unit, and resulting output power, graphed in red. The buoy was on a test bed and actuated by hand for this test.*

2.1.1. Four-Motor Generator.

The four motors were connected in a series circuit and then tested with different loads to determine the ideal load of the system. Figure 4 shows the cumulative energy produced (Joules) over time by three different loads: 48 Ohms (blue graph), 84 Ohms (red graph), and 184 Ohms (yellow graph). 84 Ohms for the 4 motors (21 Ohms for each), will produce the most energy compared to the other load values.

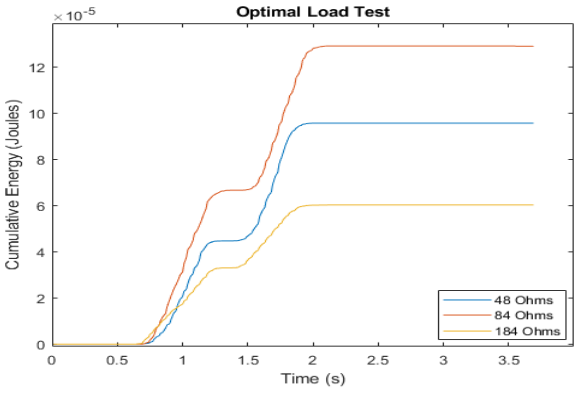

Fig. 4. Power output with three different load resistors, and constant mechanical input. *Motor DC resistance was measured to be approximately 21 ohms each. As shown, power is maximized when the load impedance matches the motor winding resistance.*

The motors were tested with both series and parallel connections in order to determine which connection would produce more power. It was determined that a series connection would yield more power output from the motors.

2.1.2. 1:2 vs 1:1 Gear System

A 3D-printed gear system, with gear ratio 1:2, was developed to compare with 1:1. Figure 5 shows the cumulative energy produced versus time for 1:2 gear system (red graph) and 1:1 gear system (blue graph). It was determined that trials with the 1:2 gear system would yield more power since it increases the revolutions per minute (RPM) of the generator gears.

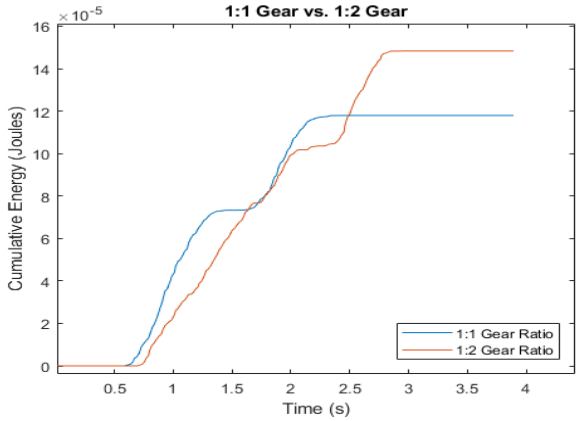

Fig. 5. 1:2 vs 1:1 gear ratio power output performance comparison. *The 1:2 gear system, graphed in red, increases the mechanical input of the motors by having twice the RPM of the 1:1 gear system, graphed in blue. This would result to a greater power output if the torque requirements are met by the buoy's lift capacity and weight.*

2.2 In-pool Testing

2.2.1. High-Pass Filtering (HPF)

Integration is used to derive motion and position information from accelerometer data. Despite normalization and using averaging to extract the accelerometer "static" rest output, after double integrating the data gathered (Bagur, 2018), the integration drift caused by the offset errors in the MPU6050s created an upward slope that prevented proper analysis of data (Kok, 2018). Figure 6 showcases the position versus time of the accelerometers integrated from the acceleration data. The increasing slope is also showed in Figure 6.

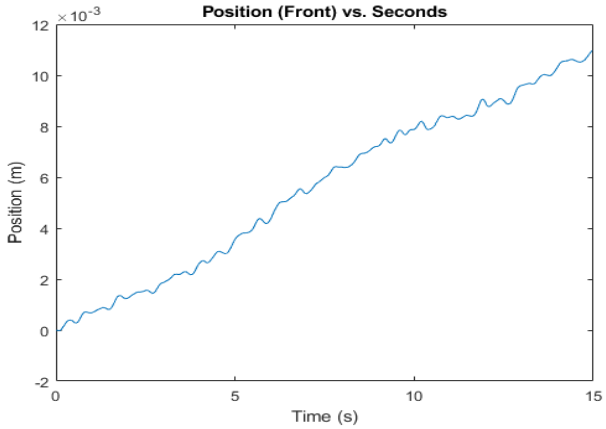

Fig. 6. Unfiltered position data (front accelerometer) showing the integration drift due to the offset errors in the MPU6050s.

A first-order Infinite-Impulse Response filter was first implemented in a spreadsheet to remove the offset errors from the data. The increasing slope was then determined and subtracted from the original data to normalize the graph. Figure 7 shows the result of this method; however, the errors are still present due to the polynomial slope in the normalized graph.

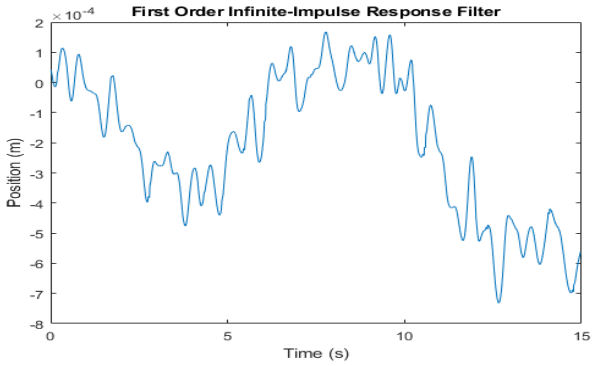

Fig. 7. A normalized first-order HPF position data. *The first order HPF was not able to remove the offset errors from the MPU6050s since the graph still exhibits a polynomial slope. This indicates the need for a higher-order HPF*

In order to remove most of the error in the data, a higher-order HPF was implemented (MathWorks, 2019). First, a Fourier Transform of the position data was initiated to determine the passband frequency of the HPF (MathWorks, 2019). Figure 8 shows that there is a small, but considerable energy content at the frequency 0.25Hz, so the passband frequency was set to this value.

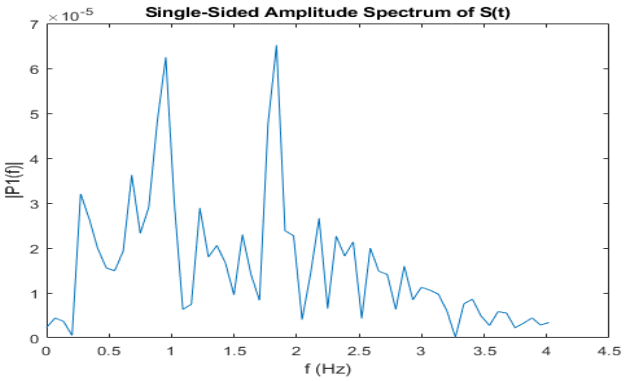

Fig. 8. Fourier transform of the position data. *This suggests a passband frequency of 0.25Hz.*

After applying the higher-order HPF, Figure 9 shows the resulting graph of the position data versus time which can now be properly analyzed and integrated.

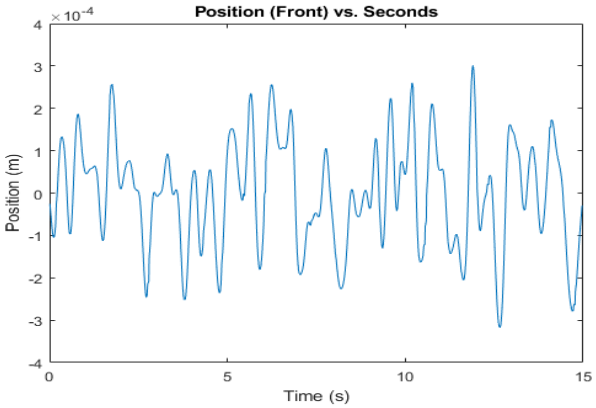

Fig. 9. Position data with higher-order HPF. *The integration drift shown in Figures 6-8 is removed and can now be properly analyzed.*

2.2.2. Wave Power

Using the filtered values, the kinetic energy absorbed by the front accelerometer, buoy, and back accelerometer was computed using Equation 1.

$$K_E = \frac{M * d^2}{no.of\ samples} \qquad \text{(Eq. 1)}$$

where:
K_E = wave power absorbed (Joules)
M = mass of the buoy (kg)
d = displacement (m)

Figure 10 shows the disparity between the wave power absorbed by the different accelerometers. The front accelerometer (blue graph) absorbed the greatest amount of wave power, followed by the buoy accelerometer (red graph) and then the back accelerometer (yellow graph). This shows that the buoy absorbed some of the wave energy before it passes to the back accelerometer.

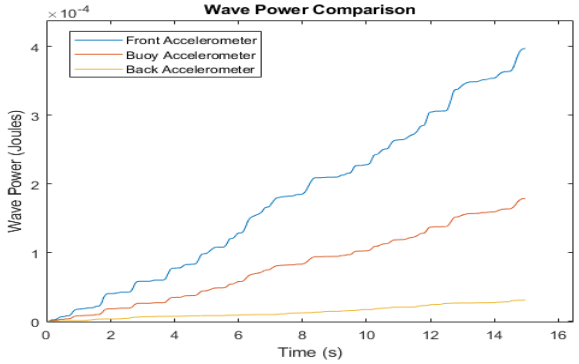

Fig. 10. Difference in wave power absorbed by accelerometers. *The disparity between the front and back accelerometers shows that the buoy absorbed some of the wave energy and the leftover unabsorbed wave was felt by the back accelerometer.*

2.2.3. Buoy Conversion Efficiency

It is seen in Figure 11 that for every wave power absorbed by the buoy, a fraction of it is converted to mechanical energy to spin the motors, and a fraction of that mechanical energy is converted into electrical energy. In order to determine the mechanical energy acquired by the motors from the wave power, Equation 2 was used.

$$M_E = \frac{P_E}{0.1517}, \qquad \text{(Eq. 2)}$$

where:
M_E = mechanical energy (Joules)
P_E = instantaneous electric power (Joules)
0.1517 = motor electrical conversion efficiency

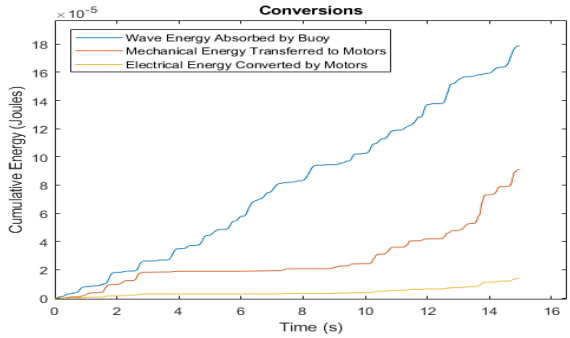

Fig. 11. Break down of the absorbed wave power (blue graph) into mechanical energy (red graph) and then electrical energy (yellow graph). *The graph shows that the absorbed wave power was not fully converted to electrical energy which indicates the presence of losses within the system.*

Using Equation 3, it was determined that the mechanical configuration of the buoy can convert an average of 37% of the wave power it absorbed.

$$Eff_M = \frac{M_E}{Absorbed\ Wave\ Power} * 100 \qquad \text{(Eq. 3)}$$

where:
Eff_M = mechanical conversion efficiency (%)

2.2.4. Losses

The developed WEC was only able to reach a mechanical conversion efficiency of 37% and an electrical conversion of 15%, which means that the buoy has characteristics that would cause the loss of energy during the conversion.

One of the main reasons for this loss is the weight of the buoy. The developed system depends on the weight of the buoy to provide the downward force that would spin-up the generators; likewise, this weight, plus the inertial weight required to spin-up the generators in the upward motion, is what the wave must lift up in order to restore the position of the buoy. In effect, the energy conversion is halved, and at least 50% of the wave energy is lost using this approach.

Another weakness of the system that would cause the loss of energy is how the generators are far from reaching their maximum rotation rate. There are four (4) limiting factors to the maximum RPM of the DC motors implemented in the prototype. First, as the rotor spins, the contacts can spark and lose good electrical contact. Second, the rotor's components have inertia; if it spins too fast, the motors can possibly end up destroying itself. Third, the back-EMF of the motor increases with RPM, and last, the winding inductance increases the impedance of the motor, limiting its power transfer as it spins faster.

Additional losses in the system includes, but are not limited to, the frictional force between the

gears, slight inaccuracy with the sensors, and gear lashing, which neglects small motions by the buoy due to the spaces between the gears.

2.2.5. Projections

If one-third of the Philippine coastline were to be filled with these buoys and run for an hour, it could power a 20-watt light bulb for 2 hours and 46 minutes factoring in the amplitude, shape, and frequency of an actual wave in the Philippines.

3. CONCLUSION

Wave energy is a renewable energy source that shows great potential; however, the complexities of designing and developing a model which can convert a near 100% of the wave power it absorbs, is hard to implement. This research is aimed to provide another design for a WEC that might eventually reach the 100%-conversion efficiency mark if further developed. This WEC model includes a linear-ratchet gear system, which converts the vertical motion of the wave into circular motion to spin the motors, a 1:2 ratio gear system to increase the mechanical input in the motors, a rectifier to convert AC into DC, and accelerometers to characterize the wave and the buoy. Currently, this model can convert 37.03% of the wave power into mechanical power which 15.17% is then converted into electric power.

In spite of its low conversion efficiency, filling one-third of the Philippines coastline with this device and letting it run for an hour, will be enough to power a 20-watt light bulb for almost 3 hours.

The losses in the system are caused by, but are not limited to, the mass of the buoy, factors that limit the RPM of the generators, the frictional force between the gears, gear lashing, and poor motor performance.

4. REFERENCES

Bagur, J.R. (2018). Trapezoidal rule: Numerical methods. Retrieved from https://dev.to/jbagur/trapezoidal-rule-numerical-methods-4fi0

Gareffa, P. What is a Continuously Variable Transmission (CVT)?. Retrieved from https://www.edmunds.com/car-technology/cvt-enters-the-mainstream.html

Kok, M., Hol, J., & Schon, T. (2018). Using inertial sensors for position and orientation estimation. Foundation and Trends in Signal Processing: Vol 11: No. 1-2, pp 1-153. Retrieved from https://arxiv.org/pdf/1704.06053.pdf

Levitan, D. (2014). Why wave power has lagged far behind as energy source. Yale Environment 360. Retrieved from. https://e360.yale.edu/features/why_wave_power_has_lagged_far_behind_as_energy_source

Lumen. (n.d.). Archimedes' principle. Retrieved from https://courses.lumenlearning.com/boundless-physics/chapter/archimedesprinciple/

MathWorks. (2019). Fourier Transform. Retrieved from https://www.mathworks.com/help/symbolic/fourier.html

MathWorks. (2019). Highpass. Retrieved from https://www.mathworks.com/help/signal/ref/highpass.html

Microchip. (2011). Op amp recfiers, peak detectors, and clamps. Retrieved from http://ww1.microchip.com/downloads/en/appnotes/01353a.pdf

Ritchie, H. & Roser, M. (2018). Energy. Our World in Data. Retrieved from https://ourworldindata.org/energy

Technology Uncorked. (2014). How to characterize a DC motor. Retrieved from https://www.tu-eshop.com/index.php?route=tublog/blog&id=19

Tofolli, A., Bitner-Gregersen, E. (2017). Type of ocean waves, waves classification. Retrieved from hps://onlinelibrary.wiley.com/doi/full/10.1002/9781118476406.emoe077

United Nations. (2019). Sustainable Development Goals. Retrieved from hps://sustainabledevelopment.un.org/?menu=1300